Journal of Magnetism and Magnetic Materials 321 (2009) 2107–2114

Contents lists available at ScienceDirect

Journal of Magnetism and Magnetic Materials

journal homepage: www.elsevier.com/locate/jmmm

Magnetic properties of stainless steels at room and cryogenic temperatures

Paul Oxley *, Jennifer Goodell, Robert Molt

Physics Department, The College of the Holy Cross, 1 College Street, Worcester, MA 01610, USA

ARTICLE INFO

Article history:
Received 10 September 2008
Received in revised form
21 November 2008
Available online 21 January 2009

PACS:
75.50.Bb

Keywords:
Magnetic measurement
Ferromagnetic property
Stainless steel
Martensitic
Ferritic

ABSTRACT

The magnetic properties of ten types of ferritic and martensitic stainless steels have been measured at room temperature and at 77 K. The steel samples studied were in the annealed state as received from the manufacturer. Our room temperature measurements indicate significantly harder magnetic properties than those quoted in the ASM International Handbook, which studied fully annealed stainless steel samples. Despite having harder magnetic properties than fully annealed steels some of the as-received steels still display soft magnetic properties adequate for magnetic applications. The carbon content of the steels was found to affect the permeability and coercive force, with lower-carbon steels displaying significantly higher permeability and lower coercive force. The decrease in coercive force with reduced carbon content is attributed to fewer carbide inclusions which inhibit domain wall motion. Cooling to 77 K resulted in harder magnetic properties. Averaged over the ten steels tested the maximum permeability decreased by 8%, the coercive force increased by 14%, and the residual and saturation flux densities increased by 4% and 3%, respectively. The change in coercive force when cooled is comparable to the theoretical prediction for iron, based on a model of domain wall motion inhibited by inclusions. The modest changes of the magnetic properties indicate that the stainless steels can still be used in magnetic applications at very low temperatures.

1. Introduction

Ferritic and martensitic steels can have good soft magnetic properties showing high permeability, low coercive force, low residual magnetic flux density, and high magnetic saturation flux density. These steels also have high electrical resistivity which is essential to minimize eddy current losses in a.c. magnet applications. The steels can be manufactured to large dimensions when required for particular applications, they can be machined easily, are widely available, and are relatively inexpensive. The combination of these properties has meant that ferritic and martensitic stainless steels have been used in a broad range of magnetic applications [1]. They can be used in fuel injectors [2] and fuel pumps on automobiles, in relays, motors, and generators, and they also have potential for use in nuclear power plants [3].

Despite the usefulness of ferritic and martensitic stainless steels in magnetic applications there has been only limited study of the magnetic properties of these steels. Most studies have used steels heat treated after purchase from the manufacturer [2,4–6]. Room temperature measurements of coercive force and maximum permeability of selected fully annealed stainless steels are also reported in the ASM Handbook published nearly 20 years ago [7]. To our knowledge no studies of the cryogenic properties of magnetic stainless steels have previously been made, although some measurements have been made with martensite austenite mixtures [8] and austenitic steels [9].

There are two main purposes of the work presented here. The first is to measure the magnetic properties of a range of magnetic stainless steels in the annealed condition as-received from the manufacturer. The magnetic properties measured are the maximum permeability (μ_{max}), the coercive force (H_c), the saturation magnetic flux density (B_s), and the residual magnetic flux density (B_r) for ten stainless steels in round rod form. The second purpose of this work is to determine how these magnetic properties change at very low temperature (77 K (−196 °C)). Magnetic stainless steels are particularly well suited to low-temperature a.c. applications since eddy current heating losses are reduced by the high electrical resistivity of the steel (typically 70 μΩ cm at room temperature and decreasing by only 40% at 77 K [10]). Minimizing heating losses is essential when working at cryogenic temperature.

2.. Experiments

The ten stainless steels tested in this study were purchased in round rod form in the annealed condition from the Fry Steel Company (Santa Fe Springs, CA). Their chemical compositions are listed in Table 1 and their rod diameters, Brinell hardnesses, and electrical resistivities are given in Table 2.

* Corresponding author. Tel.: +1 508 793 2473; fax: +1 508 793 3367.
E-mail address: poxley@holycross.edu (P. Oxley).

0304-8853/$ - see front matter © 2009 Elsevier B.V. All rights reserved.
doi:10.1016/j.jmmm.2009.01.002

Table 1
Chemical composition of the stainless steels used in this study as provided by the manufacturer.

Steel	Type	Chemical composition (% by weight)								
		Cr	C	Mn	Si	S	P	N	Ni	Mo
410	M	11.7	0.13	0.45	0.28	0.003	0.019	0.047	0.27	0.14
416	M	12.2	0.12	1.14	0.45	0.32	0.017	0.026	0.15	0.11
420	M	12.2	0.34	0.45	0.32	0.001	0.16	0.053	0.47	0.07
422	M	11.7	0.21	0.07	0.40	0.001	0.016	0.029	0.83	1.05
431	M	16.1	0.16	0.64	0.39	0.02	0.024		2.18	0.05
440A	M	15.1	0.55	0.78	0.40	0.005	0.019	0.038	0.38	0.04
430	F	16.4	0.017	0.43	0.27	0.008	0.023	0.019	0.18	0.02
430F	F	17.5	0.027	0.45	0.40	0.34	0.027	0.043	0.34	0.36
430FR	F	17.6	0.029	0.42	1.34	0.31	0.014		0.13	0.31
446	F	25.8	0.063	0.72	0.53	0.001	0.024	0.067		

Type M = martensitic, F = ferritic.

Table 2
Physical properties of the stainless steels used in this study hardness values are quoted by the manufacturer.

Steel	Diameter (inch)	Brinell hardness (HB)	Electrical resistivity (μΩ cm) [11]
410	0.188	180	57
416	0.188	235	57
420	0.188	279	55
422	0.188	215	61
431	0.265	270	72
440A	0.188	222	60
430	0.188	153	60
430F	0.188	184	60[a]
430FR	0.281	162	76[a]
446	0.315	217	64

[a] Indicates resistivity value from Dietrich [7].

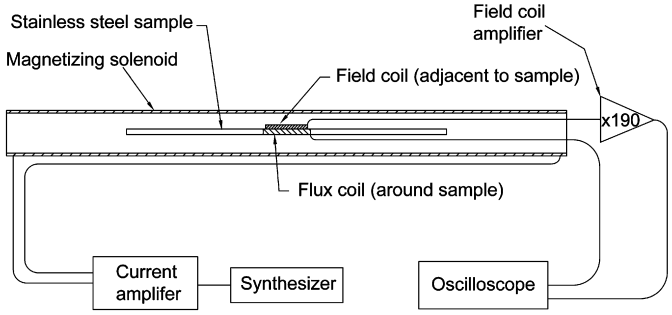

Fig. 1. Experimental apparatus used to measure the magnetic properties of stainless steel rod samples. An a.c. current in the magnetizing solenoid produces an oscillating magnetic field at the rod sample. The magnetic field is found by integrating the amplified e.m.f. induced in the field coil and the magnetic flux density is found by integrating the e.m.f. induced in the flux coil. From these measurements the magnetic properties of the rods are calculated.

The experimental arrangement used to determine the magnetic properties of the rod samples is illustrated in Fig. 1. A 30-cm-long rod sample was placed inside a 52-cm-long magnetizing solenoid. Around the rod was wound a flux coil with N_B turns and cross-sectional area A_B, and adjacent to this was the field coil with N_H turns and cross sectional area A_H. Both the flux and field coils were 3 cm long. A synthesizer controlled a home-built current amplifier to produce an oscillating current in the magnetizing coil which generated an oscillating field, H, at the sample location. The e.m.f. induced in the flux coil, ε_B, was recorded with a digital oscilloscope and the magnetic flux density, B, is calculated by

$$B(t) = \frac{1}{N_B A_B}\int_0^t \varepsilon_B\, dt \tag{1}$$

Due to the small size of the e.m.f. induced in the field coil, ε_H, this e.m.f. was amplified by a factor of 190 before being recorded by the oscilloscope. The magnetic field strength, H, is calculated by

$$H(t) = \frac{1}{\mu_0 N_H A_H}\int_0^t \varepsilon_H\, dt \tag{2}$$

In all experiments: $N_H = 300$ turns, $A_H = 4\times10^{-5}\,\mathrm{m}^2$, $N_B = 100$ turns, and A_B was equal to the cross-sectional area of the rod under test. The current in the magnetizing solenoid oscillated at a frequency of 4 Hz and could produce magnetic fields up to 4600 A/m which were sufficient to bring the rod samples close to saturation. A frequency of 4 Hz was chosen since this was high enough to provide sufficiently large e.m.f's to allow reliable measurement of $B(t)$ and $H(t)$, and was low enough to accurately give the d.c. magnetic properties. Prior to taking measurements in this way each sample was demagnetized by slowly reducing the amplitude of a 4 Hz applied field from 5400 A/m to zero. For different current amplitudes and, therefore, different applied magnetic fields a series of hysteresis loops could then be measured. A single hysteresis loop for the 430 stainless steel is shown in Fig. 2. The tips of several loops with different applied field amplitudes can be joined to produce the magnetization curve for the sample, as seen in Fig. 3 for the 430 steel. From the magnetization curve the maximum permeability, $\mu_{\max}$, is found simply from the maximum value of the quantity $B/\mu_0 H$, as

$$\mu_{\max} = \left.\frac{B}{\mu_0 H}\right|_{\max} \tag{3}$$

Values for H_c and B_r were found from hysteresis loops in which the sample reached a magnetic flux density of 1.00 T. A value for the saturation magnetic flux density, B_s, was calculated by finding the value of B at which the slope of the magnetization curve equaled μ_0, i.e.,

$$\text{at } B = B_s: \quad \frac{dB}{d(\mu_0 H)} = 1 \tag{4}$$

Since the samples were not driven fully into saturation linear extrapolation was used to infer the flux density at which Eq. (4) was satisfied (Fig. 4). Measurements of the magnetic properties at cryogenic temperatures were made in exactly the same way as at room temperature, except that the magnetizing solenoid, steel sample, and flux and field coils were cooled in liquid nitrogen.

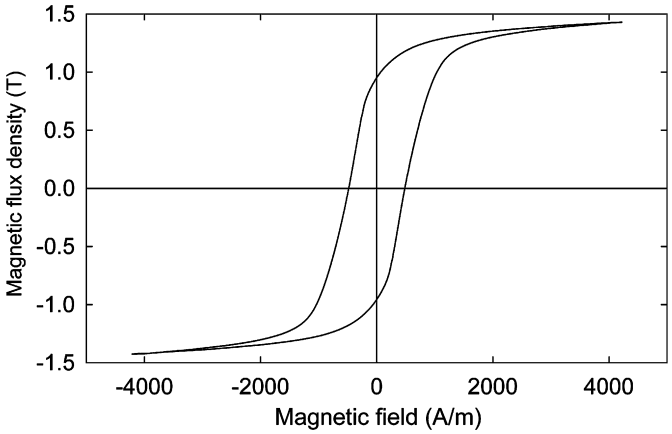

Fig. 2. Room-temperature hysteresis loop for the 430 stainless steel sample at magnetic fields up to 4200 A/m.

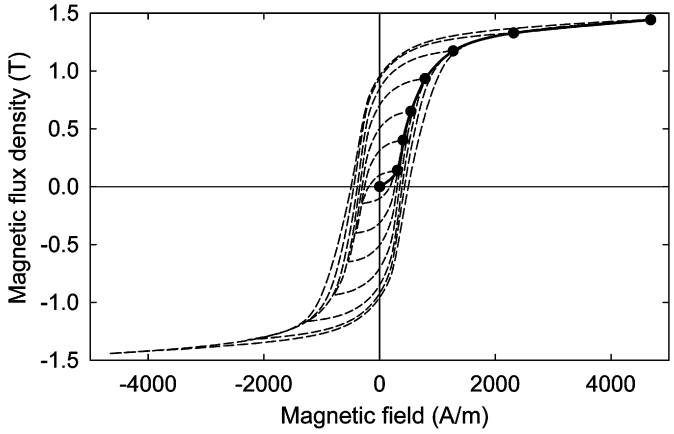

Fig. 3. Room-temperature magnetization curve (solid line) for the 430 stainless steel sample. The tips of the hysteresis loops (dashed lines) are joined to produce the magnetization curve. For clarity only some of the measured hysteresis loops are shown.

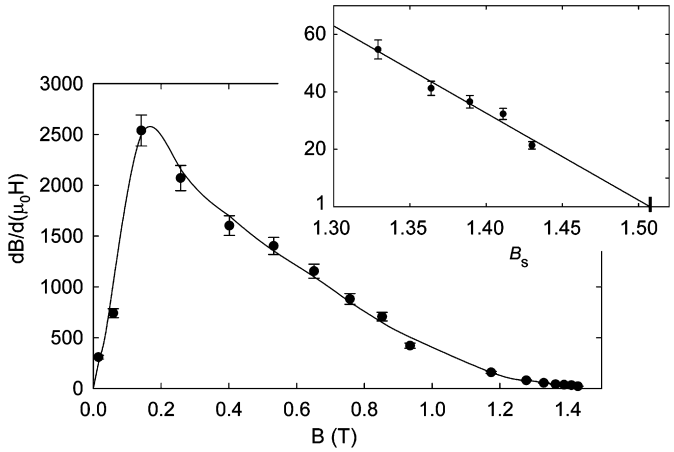

Fig. 4. Variation of the quantity $dB/d(\mu_0 H)$ with magnetic flux density at room temperature for the 430 stainless steel sample. The saturation flux density (B_s) is defined as the flux density at which $dB/d(\mu_0 H)$ is equal to one. The inset shows a linear fit to the last five data points and the extrapolation of the fit to determine a value for B_s of 1.51 T for the 430 sample.

Two additional experiments were also performed. In the first values of μ_{max} were measured for the 430FR sample with applied magnetic fields oscillating at frequencies in the range 2–30 Hz, instead of simply at 4 Hz as was used for all other data. The purpose of this test was to probe how eddy current shielding affects the measured magnetic permeability and confirm that our 4 Hz measurements correctly represent the d.c. magnetic permeabilities of the steels. The second additional experiment was to anneal the type 430 and 430F samples to 780 °C ourselves and compare their magnetic properties to those steels in the as-received condition and to those listed in the ASM International Handbook.

3.. Results and discussion

3.1. Room-temperature tests

Our measured values of μ_{max}, H_c, B_r, and B_s at room temperature and 77 K are shown in Figs. 5–8 and we begin by discussing the room-temperature results. Considering all four magnetic properties measured at room temperature the softest magnetic material was the 430FR sample. It had a maximum permeability of 960, a coercive force of 265 A/m, a residual magnetic flux density of 0.49 T, and a saturation magnetic flux

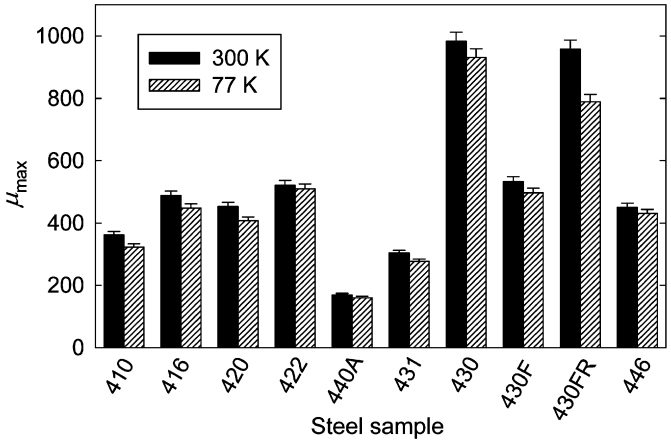

Fig. 5. 300 and 77 K values of maximum permeability for all ten steel samples tested. The error bars represent the typical variation in the measured permeability for multiple measurements.

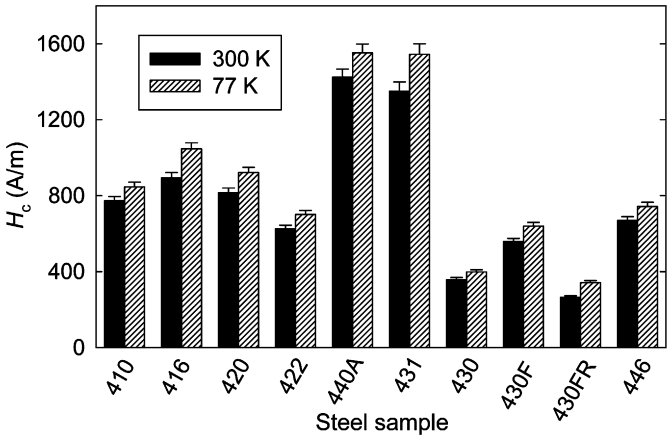

Fig. 6. 300 and 77 K values of coercive force for all ten steel samples tested. The error bars represent the typical variation in the measured coercive force for multiple measurements.

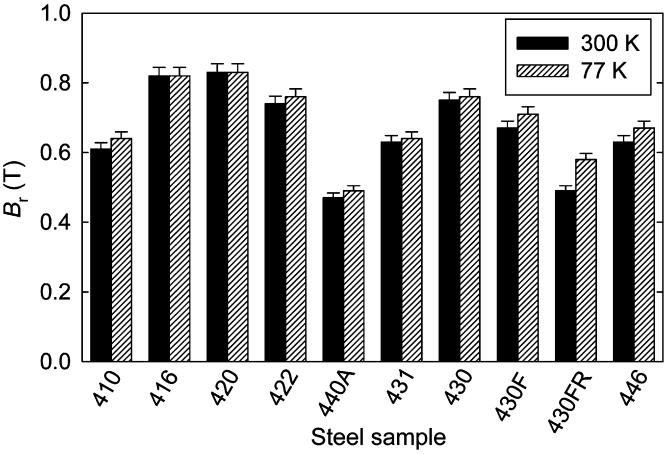

Fig. 7. 300 and 77 K values of residual flux density for all ten steel samples tested. The error bars represent the typical variation in the measured residual flux density for multiple measurements.

density of 1.47 T. Type 430FR stainless steel is designed to have good soft magnetic properties and an especially low residual flux density [12], as we observed. Type 430FR also has the highest electrical resistivity (see Table 2) of any of the steels tested due to its high silicon content. Type 430FR steel would therefore be preferred for a.c. applications where eddy current losses are a particular concern.

Exact comparisons between the measured magnetic properties of the steels are difficult due to different trace element levels and thermo-mechanical histories of our samples. However, two general trends can be identified and understood. Firstly, we observed a trend for the stainless steels with higher carbon content to have increased coercive forces and lower maximum permeabilities, as shown in Fig. 9. We interpret these changes as due to higher concentrations of chromium carbide inclusions present in higher carbon steels. These inclusions inhibit domain wall motion leading to harder magnetic properties. The influence of inclusions on the coercive force of ferromagnetic materials has been studied by many researchers [13–16]. Domain wall motion is resisted by inclusions for three reasons. Firstly, the wall area and therefore wall energy is reduced when it resides on an inclusion (the "surface tension" effect) [13]. Secondly, the intersection of a wall at an inclusion site allows a rearrangement of magnetic poles which reduces the energy of the poles [17]. Thirdly, when the inclusion is several times the wall thickness (~0.1 μm for iron), spiked closure domains form around the inclusion. These domains act to reduce the free pole energy at the inclusion, but they also inhibit wall motion [14,16–18]. In annealed stainless steels coarse carbides are significantly larger than 0.1 μm [19]. For these large inclusions spike domains, rather than the surface tension effect, is the dominant effect inhibiting wall motion and the coercive force is proportional to the volume fraction of inclusions [14]. In Fig. 9, a linear fit to the variation of coercive force with carbon content shows reasonable agreement. In Section 3.2, we also interpret changes in coercive force at low temperature with decreased wall mobility.

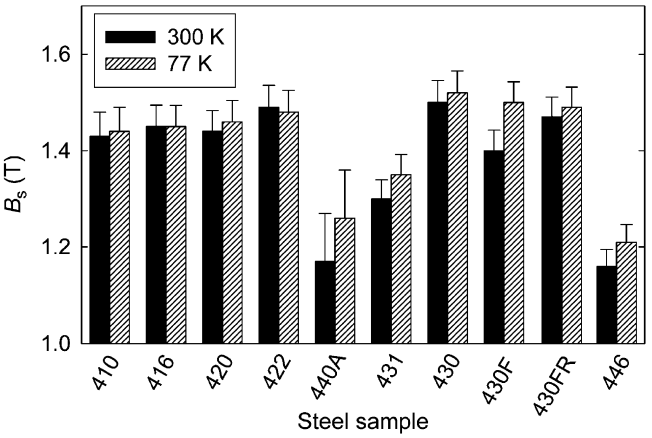

Fig. 8. 300 and 77 K values of saturation flux density for all ten steel samples tested. The error bars represent the typical variation in the measured saturation flux density for multiple measurements and the uncertainty in the extrapolation to complete saturation.

The effect of carbon on the magnetic properties of iron-carbon alloys has previously been measured [20–22]. These experiments showed that as carbon content is increased permeability decreases, coercive force increases, while residual flux density remains largely unchanged. These three dependencies are also found in our tests of stainless steels and are seen in Fig. 9. Experimentally, we found that saturation flux density is unaffected by carbon content. This is expected since saturation flux density is a structure insensitive property, little affected by the presence of trace elements, such as the low levels of carbon in our steels.

The second general trend we have observed is a reduction of saturation flux density with chromium content. This reduction has previously been reported for ferritic stainless steels [1] and for iron chromium alloys [23] and in both cases a linear decrease in saturation flux density was observed. Our data, displaying an approximate linear dependence, is shown in Fig. 10. To reduce the influence of differing carbon contents on B_s two graphs are shown in Fig. 10, one for the ferritic steels with low carbon content and one for the martensitic, higher carbon steels. Since the chromium provides stainless steel with its corrosion resistance, any given magnetic application in a corrosive environment should balance increased corrosion resistance against reduced saturation flux density.

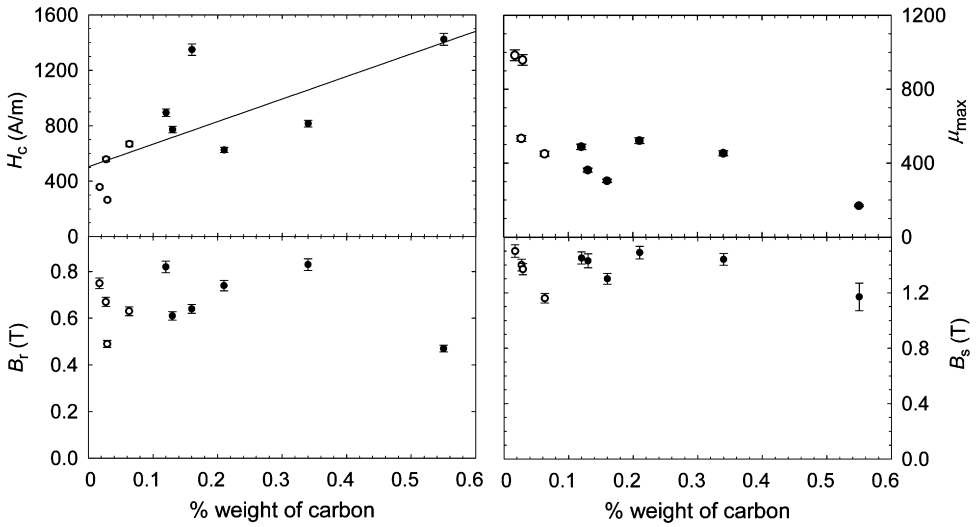

Fig. 9. Magnetic softness, as determined by a high permeability μ_{max} and a low coercive force H_c, increases with reduced carbon content. The solid line in the coercive force graph is a linear fit to the data, as predicted if coercive force is determined by large inclusions [14]. Residual and saturation flux densities (B_r and B_s) are seen to be insensitive to carbon content up to a value of 0.55% by weight, the maximum carbon content of any of the steels tested. The ferritic steels are the four data points with the lowest carbon contents and are indicated by the hollow points. The measurements were taken at room temperature and each data point represents one of the stainless steel samples tested.

Values for μ_{max} and H_c for a subset of the steels tested here are also listed in the ASM International Handbook [7] and a comparison of the two sets of measurements is made in Table 3. As can be seen in the table our measurements display lower permeability and higher coercive force than those in the ASM Handbook. The major difference between the two studies is the heat treatment performed on the steels prior to testing: the ASM Handbook samples were fully annealed while our samples were tested in the annealed state as received from the manufacturer (process annealed).

During full annealing the steel is heated to a temperature above the critical point where an austenite phase in the iron occurs. This dramatically increases the solubility of carbon in the iron's ferrite phase [24] and relieves internal strains which would otherwise impede magnetic domain wall motion. It can also increase grain size and so reduce grain boundary resistance to wall motion. Upon slow cooling a low density of coarse chromium carbides form, which inhibit domain wall motion less than a high density of fine carbides which typically exist before annealing. A process anneal does not raise the steel temperature high enough to enter the austenite phase, and hence does not reach as high a level of carbon solubility as does a full anneal. This leads to finer carbides and harder magnetic properties than fully annealed steels. This is observed in Table 3 where the process annealed steels used in this work display harder magnetic properties than the fully annealed steels in the ASM study.

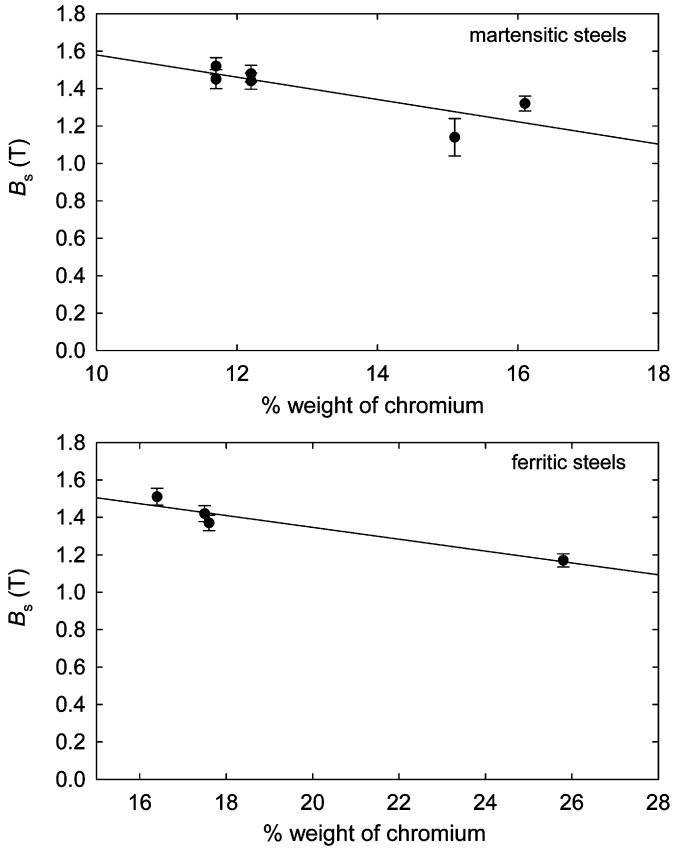

Fig. 10. Dependence of saturation flux density on chromium content for martensitic steels and ferritic steels. Each data point represents one of the stainless steel samples tested and the solid lines are linear fits to the data. An approximate linear dependence is seen, as has been previously observed [1]. The measurements were taken at room temperature.

If the softer magnetic properties of the steels listed in the ASM Handbook are to be attributed to the full annealing cycle undergone by the ASM steels, then we would expect those steels to also be mechanically softer than the steels tested in our work. This is because the more homogenous, coarser carbide microstructure produced by full annealing resists mechanical deformation less than the finer microstructure of process annealed steels. Experimentally there is clear evidence that magnetic hardness of stainless steels is correlated with mechanical hardness [3,5,25,26]. Table 3 shows that, indeed, in every case the steels reported in the ASM Handbook have a lower Brinell hardness than the steels tested in our work. The magnetic properties of as-received annealed stainless steels presented in our work, therefore, supplement and extend those of fully annealed steels listed in the ASM Handbook. Anyone wishing to use magnetic stainless steels without the inconvenience of performing a full anneal should, therefore, look to our results for information on their expected magnetic properties.

Two additional samples of our 430 and 430F steels were annealed after purchase in order to compare to the fully annealed ASM samples. The 430 and 430F steel samples were chosen for annealing since they have the lowest annealing temperature of any of the steels tested and therefore took the shortest time to anneal. Even so, the annealing process required a full day to complete. The steel samples were heated to 780 °C in a hydrogen atmosphere, held at this temperature for 1 h, and then cooled to 600 °C at a rate of 36 °C per hour. They were then air cooled. Fig. 11 shows how μ_{max} and H_c are changed by the additional annealing heat treatment. A substantial improvement results, with approximately a factor of two increase in μ_{max} and a factor of two decrease in H_c for both types of steel. After this additional annealing our 430F sample did not display as soft magnetic properties as the 430F sample quoted in the ASM Handbook. Our 430 sample did, however, achieve similar magnetic properties as the Handbook 430F sample (the Handbook does not provide data for 430 steel). The main difference between these two types of steel is that type 430F has a greater amount of sulfur, which should little affect the magnetic properties. We conclude then that additional annealing of as-received steels can provide as soft magnetic properties as those of fully annealed steels in the ASM Handbook. We presume that our 430F sample remained

Table 3
Comparison of the maximum permeability and coercive force for the stainless steels used in this work and in the ASM Handbook [7].

Steel	μ_{max} (this work)	μ_{max} (ASM)	H_c (this work)	H_c (ASM)	Brinell hardness (this work)	Brinell hardness (ASM)
410	360	750	770	480	180	163
416	490	750	900	480	235	163
420	450	950	820	800	279	183
430F	530	2000	560	160	184	140
430FR	960	2600	270	130	162	153
446	450	1000	670	360	217	163

Also shown is the mechanical hardness of the steel samples used. In this work the mechanical hardness was measured and provided by the steel manufacturer. The steels tested in this work display harder magnetic and mechanical properties than those in the ASM Handbook due to their different annealing procedures.

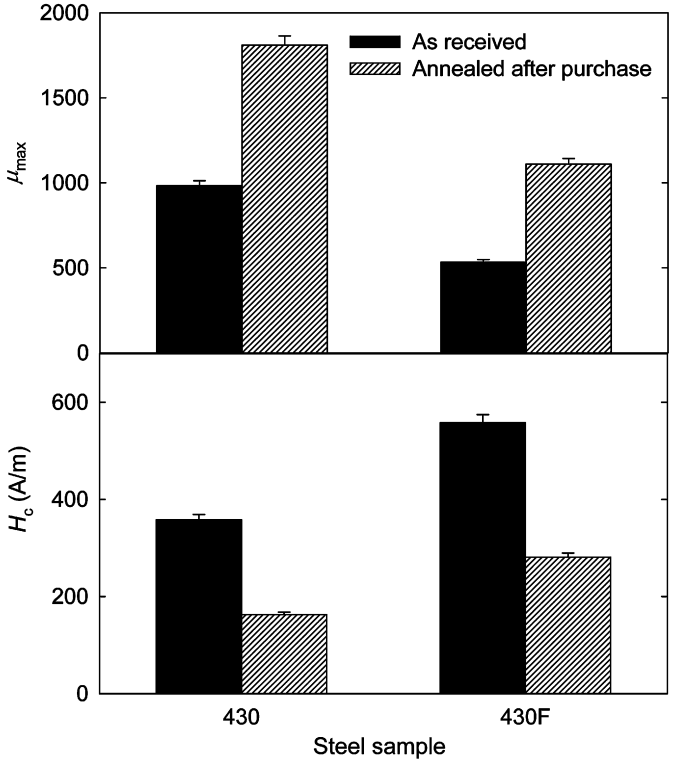

Fig. 11. Effect of annealing two of the as-received samples at 780 °C and cooling slowly. Substantially softer magnetic properties result and the 430 sample is as soft as the fully annealed 430F sample listed in the ASM Handbook. The measurements were taken at room temperature.

magnetically harder than our 430 sample due to its higher initial mechanical hardness and carbon content (Tables 1 and 2).

One final test was performed at room temperature to measure μ_{max} of the 430FR sample with applied magnetic fields oscillating at frequencies in the range 2–30 Hz, instead of simply at 4 Hz as was used for all data previously mentioned. The purpose of this test was two-fold: firstly to probe how eddy current shielding affects the measured magnetic properties when the steels are used in low-frequency a.c. applications, and secondly to confirm that 4 Hz measurements accurately represent the d.c. magnetic properties. Eddy current shielding of the applied magnetic field in the interior of the steel rods leads to an effective permeability, μ', which is lower than the d.c. permeability, μ. The theoretical relationship between μ and μ' is given by [20]

$$\frac{\mu'}{\mu} = \frac{2}{\phi}\left(\frac{Ber(\phi)\times Bei'(\phi) - Bei(\phi)\times Ber'(\phi)}{Ber^2(\phi)+Bei^2(\phi)}\right) \tag{5}$$

where $\phi = d\sqrt{\pi\mu_0\mu f/2\rho}$, d is the rod diameter, f is the frequency of the applied field, and ρ is the electrical resistivity of the steel. The Kelvin functions *Ber, Bei, Ber′*, and *Bei′* are given by

$$Ber(\phi) = \sum_{n=0}^{\infty}\frac{1}{[(2n)!]^2}\left(\frac{\phi}{2}\right)^{4n}(-1)^n$$

$$Bei(\phi) = \sum_{n=0}^{\infty}\frac{1}{[(2n+1)!]^2}\left(\frac{\phi}{2}\right)^{4n+2}(-1)^n$$

$$Ber'(\phi) = \sum_{n=0}^{\infty}\frac{2n}{[(2n)!]^2}\left(\frac{\phi}{2}\right)^{4n-1}(-1)^n$$

$$Bei'(\phi) = \sum_{n=0}^{\infty}\frac{2n+1}{[(2n+1)!]^2}\left(\frac{\phi}{2}\right)^{4n+1}(-1)^n \tag{6}$$

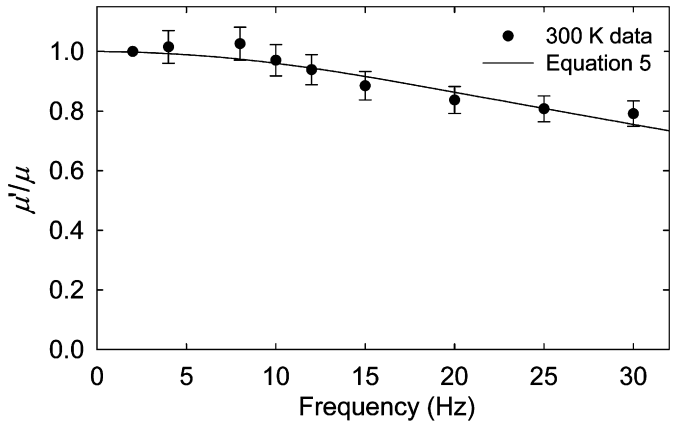

Fig. 12. Variation of μ_{max} with the frequency of the applied magnetic field, normalized to the value of μ_{max} at 2 Hz (data points). The solid line is the prediction of Eq. (5) and is not a fit to the data. As the field frequency is increased eddy currents lead to a reduction in the measured permeability, in agreement with the theoretical prediction. At a frequency of 60 Hz, Eq. (5) predicts an effective permeability equal to 50% of the d.c. permeability.

A comparison between Eq. (5) and our measurements of the variation of μ_{max} with frequency for the as-received 430FR sample is shown in Fig. 12. In our data the d.c. permeability, μ, is taken to be the permeability measured at the lowest frequency used, i.e., 2 Hz. There is good agreement between the theory and the experiment, both indicating a reduction in permeability as the frequency of the applied field is increased. Whether or not this reduction is acceptable will depend on the specific magnetic application. This data and the theory also confirm that our measurements using a 4 Hz oscillating field accurately represent the d.c. magnetic permeabilities of our stainless steels since the 4 Hz data point is in good agreement with the d.c. value.

3.2. Cryogenic tests

At 77 K the steels displayed harder magnetic properties than at 300 K, as shown in Figs. 5 to 8. On average over the ten steels tested there was a decrease in μ_{max} of 8%, an increase in H_c of 14%, an increase in B_r of 4%, and an increase in B_s of 3% when the steels were cooled to 77 K. These modest changes in magnetic properties indicate that the stainless steels can still be used in magnetic applications at very low temperature.

In Section 3.1, we discussed how an increase in coercive force with carbon content can be interpreted in terms of large carbide inclusions which impede domain wall motion. Now we seek to interpret how temperature affects coercive force, again based on a model of domain wall motion impeded by large inclusions. The coercive force due to large inclusions around which closure domains exist is proportional to the domain wall energy, E_w, and inversely proportional to the saturation magnetization, M_s [14,15]:

$$H_c \propto \frac{E_w}{M_s} \tag{7}$$

At a domain wall the magnetization vector must change direction, and since crystal anisotropy energy depends on the orientation of the magnetization vector relative to the crystal's easy axis there is an energy associated with this direction change. Domain wall energy, therefore, depends on the crystal anisotropy through the anisotropy constant, K, which is temperature dependent. The wall energy also depends on the stress in the material and the material's magnetostriction constant, λ, but this contribution is usually considered small for iron [14,15]. The

domain wall energy is, therefore, given by

$$E_w \propto \sqrt{K(T)} \tag{8}$$

The Akulov–Zener law for the variation of $K(T)$ with temperature is given by [27]

$$K(T) = K_0\left(\frac{M_s(T)}{M_{s0}}\right)^{10} \tag{9}$$

for a cubic material such as iron. K_0 and M_{s0} are the anisotropy constant and saturation magnetization at absolute zero, and $M_s(T)$ is the saturation magnetization at temperature T. The temperature dependence of M_s is given by Bloch's $T^{3/2}$ law [28]

$$M_s(T) = M_{s0}\left[1 - A\left(\frac{T}{\theta}\right)^{3/2}\right] \tag{10}$$

where θ is the Curie temperature and the constant A has an empirical value of 0.118 for iron [20]. Strictly, Eq. (10) is only valid at temperatures near absolute zero, however it has been tested for iron and nickel and the $T^{3/2}$ scaling was confirmed up to temperatures as high as 300 K [20]. Gathering together Eqs. (7)–(10) the temperature dependence of the coercive force is given by

$$H_c(T) \propto M_s^4(T) \propto \left[1 - A\left(\frac{T}{\theta}\right)^{3/2}\right]^4 \tag{11}$$

Applying Eq. (11) for iron we find

$$\frac{H_c(T=77)}{H_c(T=300)} = 1.07 \tag{12}$$

An additional temperature-dependent contribution to H_c, not included in Eq. (11), is that from grain boundaries. This contribution is proportional to $M_s(T)$ and gives rise to an increase of 2% above the value in Eq. (12) for iron [15]. Averaged over the ten steels we tested the ratio of the coercive force at 77 K to the coercive force at 300 K was 1.14. Given the complexity of the microstructure of stainless steels in comparison with iron and given the inherent difficulties of interpreting macroscopic properties from microscopic effects, we consider the agreement between the theory of Eq. (11) and experiment to be fair. Neglected in the theory of Eq. (11) is any contribution to the coercive force from internal stresses which inhibit wall motion. These stresses are produced by crystal dislocations and inclusions and may not be negligible in our steels as they are in iron. Whether or not these will give rise to a temperature-dependent coercive force is not clear however. The magnetostriction constant λ_{100} of iron has negligible change between room temperature and 77 K [29], and so for iron one would not expect a change in H_c with temperature due to stress.

Eq. (10) predicts a 2% increase in saturation magnetization for iron when cooled to 77 K. This increase is close to the average measured increase in B_s, for the ten steels tested. The measured increase was 2.6 (1.3)%, where the number in parenthesis represents the uncertainty in the average measurement due to the $\pm 4\%$ uncertainty in each of the ten individual measurements of B_s. The measurements of saturation flux density in our steels, therefore, agree with the theoretical prediction for iron.

Previous measurements of the temperature dependence of the coercive force for materials more similar to stainless steel than iron are not numerous. Experiments on iron–chromium alloys [23] show a change in M_s by a factor of 1.03 between room temperature and 77 K for 15 at% Cr. When raised to the fourth power as in Eq. (11) this indicates a 13% increase in H_c at 77 K. The only previous measurements of the temperature dependence of the magnetic properties of magnetic steels that we have found can be inferred from measurements of the coercive force of martensite/austenite two phase steels [8]. In that study, the coercive force of a mixture containing 36% martensite was observed to increase by approximately 15% when the mixture was cooled from 300 to 80 K. Our results for the change in coercive force with temperature are, therefore, consistent with these previous experiments. To our knowledge our study is the first comprehensive set of experiments investigating the low temperature magnetic properties of magnetic stainless steels.

4.. Conclusions

We have measured the magnetic properties of a range of ferritic and martensitic stainless steels and studied how these properties are affected by cooling to 77 K. This work provides information about the four most important magnetic parameters (μ_{max}, H_c, B_s, and B_r) which can be used when selecting stainless steels for particular magnet applications. A typical application of this information would be when choosing a steel to construct an electromagnet in which minimizing eddy current losses is important. We tested steels in the as-received annealed condition and so our work would be particularly important for researchers who wish to use magnetic steels but who cannot, or, for convenience, do not wish to fully anneal the steels after purchase. The modest changes in the magnetic properties we observe when the steels are cooled to 77 K indicate that they can still be used in magnetic applications at very low temperatures, and our results provide information as to their expected low-temperature magnetic properties.

Acknowledgements

The authors wish to thank John Oxley for constructing the current and field coil amplifiers, Dick Miller for machining expertise used in constructing the experimental set up, and Drs. Alan Fox and De-Ping Yang for useful discussions and for reading the manuscript. We thank the referee for their helpful comments on the manuscript. We also thank the Research Corporation for funding through Cottrell College Science Award CC6761.

References

[1] D.A. DeAntonio, Adv. Mater. Process. 161 (2003) 29.
[2] L. Battistini, R. Benasciutti, A. Tassi, J. Mag. Magn. Mater. 133 (1994) 603.
[3] K. Ara, N. Ebine, N. Nakajima, ASME Trans. J. Pressure Vessel Technol. 118 (1996) 447.
[4] K. Ara, IEEE Trans. Magn. 25 (1989) 2617.
[5] H. Kwun, G.L. Burkhardt, J. Appl. Phys. 15 (1987) 1576.
[6] S.S.M. Tavares, D. Fruchart, S. Miraglia, D. Laborie, J. Alloys Compd. 312 (2000) 307.
[7] Douglas W. Dietrich, Magnetically Soft Materials, ASM Handbook, vol. 2, Properties and Selection: Nonferrous Alloys and Special-Purpose Materials, ASM, Materials Park, OH, 1990.
[8] J. Ding, H. Huang, P.G. McCormick, R. Street, J. Mag. Magn. Mater. 139 (1995) 109.
[9] D.C. Larbalestier, H.W. King, Cryogenics 13 (1973) 160.
[10] J.E. Jensen, W.A. Tuttle, R.B. Stewart, H. Brechna, A.G. Prodell (Ed.), Brookhaven National Laboratory Selected Cryogenic Data Notebook, Brookhaven National Laboratory Report Number, BNL-10200-R, 1980.
[11] Philip Harvey (Ed.), Engineering Properties of Steel, ASM, Materials Park, OH, 1982.
[12] Gunvant N. Maniar, Terry A. DeBold, Technical Article 00002, Carpenter Technology Corporation, Reading, PA, 1997.
[13] M. Kersten, Z. Physik 44 (1943) 63.
[14] L.J. Dijkstra, C. Wert, Phys. Rev. 76 (1950) 979.
[15] John B. Goodenough, Phys. Rev. 95 (1954) 917.
[16] William D. Nix, Robert A. Huggins, Phys. Rev. 135 (1964) A401.
[17] L. Néel, Cah. Phys. 25 (1944) 21.
[18] H.J. Williams, Phys. Rev. 71 (1947) 646.
[19] J.R. Davis, Stainless Steels ASM Specialty Handbook, ASM, Materials Park, OH, 1994.

[20] R.M. Bozorth, Ferromagnetism, D. Van Nostrand Company, New York, 1961.
[21] E. Gumlich, Wiss. Abhandl. Physik-tech. Reichsanstalt 4 (1918) 267.
[22] T.D. Yensen, Trans. Am. Inst. Elec. Eng. 43 (1924) 145.
[23] A.T. Aldred, Phys. Rev. B 14 (1976) 219.
[24] B.L. Bramfitt, 3rd Ed, Carbon and Alloy Steels Mechanical Engineers Handbook, vol. 1, Wiley, Hoboken, NJ, 2006.
[25] Noriya Ebine, Katsuyuki Ara, IEEE Trans. Magn. 35 (1999) 3928.
[26] P.D.S. Pedrosa, J.R. Teodosio, S.S.M. Tavares, J.M. Neto, M.R. da Silva, J. Alloys Compd. 329 (2001) L14.
[27] C. Zener, Phys. Rev. 96 (1954) 1335.
[28] F. Bloch, Z. Phys. 61 (1930) 206.
[29] G.M. Williams, A.S. Pavlovic, J. Appl. Phys. 39 (1968) 571.